H_∞ Preview Control for Automatic Carrier Landing

FARHAN Masood[1], *XUE Yixuan*[1], *ZHEN Ziyang*[1,2*], *YANG Liuqing*[1]

1. College of Automation Engineering, Nanjing University of Aeronautics and Astronautics, Nanjing 211106, P. R. China;
2. Jiangsu Key Laboratory of Internet of Things and Control Technologies, Nanjing 210016, P. R. China

(Received 5 December 2017; revised 5 May 2018; accepted 15 June 2019)

Abstract: This paper focuses on the application of H_∞ preview control in automatic carrier landing system (ACLS) for carrier-based aircraft. Due to the mutual movement between aircraft and carrier, the landing process becomes considerably more challenging compared to a conventional runway landing. ACLS systems mitigate this by predicting deck motion and generating ideal glide slope path for tracking. Although, this predicted glide slope information is available in advance, conventional control structures are still unable to use this future information. H_∞ preview control has the ability to utilize this future information for improving tracking response and disturbance rejection. The process of incorporating preview information into ACLS framework and synthesizing the H_∞ preview controller is presented. The methodology is verified using the example of F/A-18 automatic carrier landing problem and results are presented.

Key words: H_∞ control; preview control; carrier-based aircraft; automatic carrier landing; robust preview control

CLC number: V249 **Document code**: A **Article ID**: 1005-1120(2019)06-0919-08

0 Introduction

One of the most demanding tasks facing a pilot is landing of an aircraft on a carrier. The rough ocean environment, a short landing strip, and movement of the carrier make carrier based landing considerably more daunting compared to landing on a stationary ground based runway[1-2]. Pitch and heave motion of the carrier, brought about by rough ocean conditions, can dramatically change the touchdown point and cause large vertical deck velocities. This can result in reducing impact velocity margins[3]. In most modern aircrafts, low speeds of approach are more prone to unstable, especially in the presence of air-wake disturbances[4-5]. The compounded effects of all these factors make the automatic carrier landing a difficult control problem with tight tracking error tolerances[6]. Automatic carrier landing system(ACLS) helps ensure the safest approach velocity and descent slope to the carrier deck and touchdown[7]. Since the ideal glide slope trajectory is already known and deck motion is predictable to some degree, ACLS becomes an ideal application for preview control[8]. Preview control utilizes this future information to greatly enhance transient response[9].

Recently, there has been an increasing interest in preview control[10-19]. One of the most popular approaches for synthesizing discrete-time optimal preview controllers is to augment the system with a delay line model and converting the preview control problem to standard H_2/H_∞ control framework[20]. A problem with this approach is that the size of associated discrete algebraic Riccati equation (DARE) increases with the increase in preview length. The usual methods of brute force optimization quickly become infeasible with longer preview lengths. This problem has been solved recently for H_2[21] and for H_∞[22]. H_2 control methods have been significantly more attractive to engineers in the past due to the difficulties associated with H_∞ based methods. Therefore most of the theoretical work on H_∞ based preview control was scattered over numerous publications. A single and generic framework for solving H_∞ preview control problems was unavailable until

*Corresponding author, E-mail address: zhenziyang@nuaa.edu.cn.

How to cite this article: FARHAN Masood, XUE Yixuan, ZHEN Ziyang, et al. H_∞ Preview Control for Automatic Carrier Landing[J]. Transactions of Nanjing University of Aeronautics and Astronautics, 2019, 36(6): 919-926.
http://dx.doi.org/10.16356/j.1005-1120.2019.06.005

recently[23]. The main contribution of this paper is to apply the techniques refined and collected for tackling H_∞ preview control problems, from an engineering point of view, to the ACLS framework. The process of adding preview to a traditional ACLS control problem and synthesis of controller using standard H_∞ control theory[24] is discussed. Finally, the methodology is verified using the example of F/A-18 automatic carrier landing problem.

1 Problem Statement

Although H_∞ preview control has considerable scope for application given the superior performance and robustness properties, the work is mostly theoretical in nature and there is a need to produce a generic set of tools for application in flight control. The aim of this work is to provide a set of practical solutions for application of H_∞ preview control to flight control by using the example of ACLS. Furthermore, the procedure of adding preview to a standard ACLS framework and converting the resulting preview control problem into standard H_∞ framework as given in Green & Limebeer[24], needs to be laid out in an application friendly manner.

2 H_∞ Preview Control Scheme

2.1 Generalized plant model

Consider the following generalized linear discrete plant model (Fig. 1), as Green & Limebeer[24]

$$\boldsymbol{G}=\begin{cases}\boldsymbol{x}(k+1)=A_g\boldsymbol{x}(k)+B_{1g}\boldsymbol{r}(k)+B_{2g}\boldsymbol{u}(k)\\ \boldsymbol{z}(k)=C_{1g}\boldsymbol{x}(k)+D_{11g}\boldsymbol{r}(k)+D_{12}\boldsymbol{u}(k)\\ \boldsymbol{y}(k)=C_{2g}\boldsymbol{x}(k)+D_{21g}\boldsymbol{r}(k)\end{cases}$$

where $\boldsymbol{x}(k)\in\mathbf{R}^{n_g}$ is the state vector, $\boldsymbol{u}(k)\in\mathbf{R}^m$ the control input, $\boldsymbol{z}(k)\in\mathbf{R}^p$ the cost output, and $\boldsymbol{y}(k)\in\mathbf{R}^{q_g}$ the measurement output of the system. Moreover, $\boldsymbol{r}(k)\in\mathbf{R}^{l_r}$ denotes the previewable exogenous signal which can be considered as reference signal or the disturbance. Let the preview length be N, i.e. the values of $\boldsymbol{r}(k),\boldsymbol{r}(k+1),\cdots,\boldsymbol{r}(k+N)$ are available for the controller.

The objective is to synthesize a controller $\boldsymbol{K}=[K_y'\ K_r']'$ which generates the control input as[20]

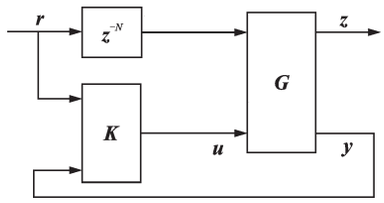

Fig.1 Generalized regulator with preview

$$\boldsymbol{u}(k)=K_y\boldsymbol{x}(k)+\sum_{i=1}^{N}K_{ri}\boldsymbol{r}(k+i) \tag{1}$$

such that $\left\|T_{r\to z}\right\|_\infty$ is minimized. The controller comprises of two parts, i.e. one feedback term and one feedforward term.

2.2 State augmentation

The procedure for converting the H_∞ preview control problem into standard H_∞ framework[20] involves augmenting the delay line model to the state space model of the system. This allows us to utilize the methods of H_∞ control theory[24] for synthesizing controller gains. Let's define

$$\boldsymbol{p}(k):=\boldsymbol{r}(k+N-1) \tag{2}$$

Let $\boldsymbol{x}_d(k)$ be the vector containing the previewed signal available for control

$$\boldsymbol{x}_d(k)=\begin{bmatrix}\boldsymbol{r}(k)\\ \boldsymbol{r}(k+1)\\ \vdots\\ \boldsymbol{r}(k+N)\end{bmatrix}=\begin{bmatrix}\boldsymbol{p}(k-N+1)\\ \boldsymbol{p}(k-N+2)\\ \vdots\\ \boldsymbol{p}(k+1)\end{bmatrix}\in\mathbf{R}^{l_r(N+1)}$$

We have

$$\boldsymbol{\phi}=\begin{cases}\boldsymbol{x}_p(k+1)=A_p\boldsymbol{x}_p(k)+B_p\boldsymbol{p}(k)\\ \boldsymbol{y}_p(k)=C_p\boldsymbol{x}_p(k)\end{cases}$$

where $\boldsymbol{\phi}$ is the system for N-step delay line and $\boldsymbol{A}_p,\boldsymbol{B}_p,\boldsymbol{C}_p$ are defined by

$$A_p=\begin{bmatrix}0 & I & & 0\\ & 0 & \ddots & \\ & & \ddots & I\\ 0 & & & 0\end{bmatrix},B_p=\begin{bmatrix}0\\ \vdots\\ 0\\ I\end{bmatrix},C_p=[I\quad 0\quad\cdots\quad 0]$$

Now, define the augmented state vector

$$\chi(k)=[\boldsymbol{x}'(k)\quad\boldsymbol{x}_p'(k)]' \tag{3}$$

The augmented system formed by combining $\boldsymbol{G}$ and $\boldsymbol{\phi}$ is given by

$$\boldsymbol{P}=\begin{cases}\chi(k+1)=\overline{A}\,\chi(k)+\overline{B}_1\boldsymbol{p}(k)+\overline{B}_2\boldsymbol{u}(k)\\ \boldsymbol{z}(k)=\overline{C}_1\chi(k)+\overline{D}_{11}\boldsymbol{p}(k)+\overline{D}_{12}\boldsymbol{u}(k)\\ \boldsymbol{y}(k)=\overline{C}_2\chi(k)+\overline{D}_{21}\boldsymbol{p}(k)\end{cases}$$

where

$$\overline{A}=\begin{bmatrix}A_g & B_{1g}C_p\\ 0 & A_p\end{bmatrix},\overline{B}_{1r}=\begin{bmatrix}0\\ B_p\end{bmatrix},\overline{B}_2=\begin{bmatrix}B_{2g}\\ 0\end{bmatrix}$$

$$\overline{C}_1=[\,C_{1g}\quad D_{11g}C_p],\overline{D}_{11}=[0],\overline{D}_{12}=[D_{12}]$$

$$\overline{C}_2=[\,C_{2g}\quad D_{21g}C_p\,],\overline{D}_{21}=[\,0\,]$$

It is clearly seen that the preview controller of Eq.(1) is a state feedback law for the augmented system $\boldsymbol{P}$. In general, the state information is available for feedback in flight control applications through the implementation of an observer. The generalized plant with preview can be represented as[24]

$$\boldsymbol{P}=\left[\begin{array}{c|cc}\overline{A} & \overline{B}_1 & \overline{B}_2\\ \overline{C}_1 & \overline{D}_{11} & \overline{D}_{12}\\ I & 0 & 0\\ 0 & I & 0\end{array}\right] \tag{4}$$

This description of the plant model is now compatible with the full information H_∞ control problem laid out in Green & Limebeer[24], and which satisfies the following assumptions: (1) $(\overline{A},\overline{B}_2)$ is stabilizable, (2) $\overline{D}'_{12}\overline{D}_{12}>0$, (3) Rank $\begin{bmatrix}\overline{A}-\mathrm{e}^{\mathrm{j}\theta}I & \overline{B}_2\\ \overline{C}_1 & \overline{D}_{12}\end{bmatrix}=n+m$, $\forall\theta\in(-\pi,\pi)$.

Now define

$$\overline{B}=[\,\overline{B}_1\quad\overline{B}_2\,]=\begin{bmatrix}0 & B_{2g}\\ B_p & 0\end{bmatrix}$$

$$\boldsymbol{L}=\begin{bmatrix}0\\ D'_{12}C_{1g}+D'_{12}D_{11g}C_p\end{bmatrix}$$

$$\boldsymbol{Q}=\overline{C}'_1\overline{C}_1=C'_{1g}C_{1g}+C'_pD'_{11g}D_{11g}C_p$$

$$\boldsymbol{R}=\begin{bmatrix}\overline{D}'_{11}\overline{D}_{11}-\gamma^2I & \overline{D}'_{11}\overline{D}_{12}\\ \overline{D}'_{12}\overline{D}_{11} & \overline{D}'_{12}\overline{D}_{12}\end{bmatrix}=\begin{bmatrix}-\gamma^2I & 0\\ 0 & D'_{12}D_{12}\end{bmatrix}$$

$$\overline{\boldsymbol{R}}=\boldsymbol{R}+\overline{B}'\boldsymbol{X}\overline{B}=\begin{bmatrix}\overline{R}_1 & \overline{R}'_2\\ \overline{R}_2 & \overline{R}_3\end{bmatrix}$$

$$\overline{\boldsymbol{L}}=\boldsymbol{L}+\overline{B}'\boldsymbol{X}\overline{A}=\begin{bmatrix}\overline{L}_1\\ \overline{L}_2\end{bmatrix}$$

Also define

$$\boldsymbol{A}_c=\overline{A}-\overline{B}\,\overline{\boldsymbol{R}}^{-1}\overline{\boldsymbol{L}}$$

In Green & Limebeer[24], it is shown that if assumptions (1)—(3) are satisfied, a stabilizing controller $\boldsymbol{K}$ of the form Eq.(1) which achieves $\|T_{r\to z}\|_\infty<\gamma$, exists, if and only if there exists a semi positive definite matrix $\boldsymbol{X}$ which solves the Discrete algebraic Riccati equation(DARE)

$$\boldsymbol{X}=\overline{\boldsymbol{A}}'\boldsymbol{X}\overline{\boldsymbol{A}}+\boldsymbol{Q}-\overline{\boldsymbol{L}}\,\overline{\boldsymbol{R}}^{-1}\overline{\boldsymbol{L}} \tag{5}$$

such that $\boldsymbol{A}_c$ is asymptotically stable and

$$\nabla=\overline{\boldsymbol{R}}_1-\overline{\boldsymbol{R}}'_2\overline{\boldsymbol{R}}_3^{-1}\overline{\boldsymbol{R}}_2 \tag{6}$$

is negative definite.

The controller $\boldsymbol{K}$ is given by

$$\boldsymbol{K}=-\overline{\boldsymbol{R}}_3^{-1}[\,\overline{\boldsymbol{L}}_2\quad\overline{\boldsymbol{R}}_2] \tag{7}$$

If Eq.(6) is negative definite, $\boldsymbol{X}$ is a feasible solution and if $\boldsymbol{A}_c$ is asymptotically stable, $\boldsymbol{X}$ is a stabilizing solution. Hence, the full information H_∞ control problem has a solution if and only if $\boldsymbol{X}$ is semi positive definite, feasible and stable[24].

By converting the preview problem into a form which is compatible with full information H_∞ control theory[24], we can utilize the powerful mathematical tools at our disposal to obtain requisite performance and fine tune close loop characteristics of the system like fast convergence, disturbance rejection, uncertainty robustness etc.

3 ACLS Framework

This section describes how to convert a traditional ACLS control problem to a preview control problem so that we may use the methods described in the previous section to obtain a H_∞ preview controller.

ACLS can be divided into two main subsystems namely the guidance system and the flight control system[25]. The guidance system generates landing commands and reference glide slope for the flight control system. The control system can be further divided into lateral control system and longitudinal control system. The preview information available for flight control system is the ideal glide slope height H_c and lateral bias Y_c. Fig.2 shows an overview of the ACLS.

3.1 Aircraft model description

The discretized linearized aircraft model has the following form

$$\boldsymbol{x}(k+1)=\boldsymbol{A}\boldsymbol{x}(k)+\boldsymbol{B}\boldsymbol{u}(k) \tag{8}$$

where the state vector is given as

$$\boldsymbol{x}=[\,\Delta\upsilon\ \Delta\alpha\ \Delta q\ \Delta\theta\ \Delta H\ \Delta\beta\ \Delta p\ \Delta r\ \Delta\phi\ \Delta\psi\quad Y\,]'$$

The individual state variables are the airspeed, angle of attack, pitch rate, pitch, altitude, sideslip

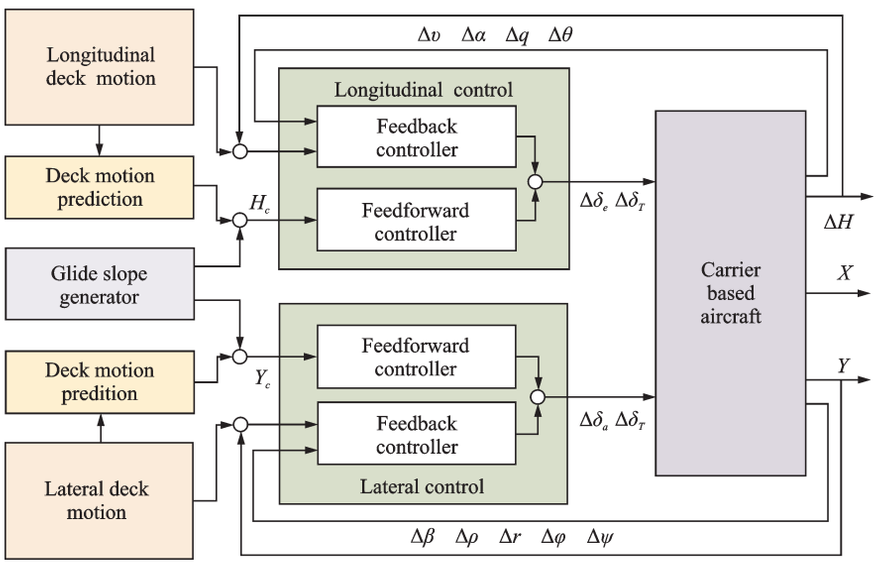

Fig.2 ACLS overview

angle, roll rate, yaw rate, roll, yaw and lateral bias respectively. The control input vector $\boldsymbol{u}=[\Delta\delta_e\ \Delta\delta_T\ \Delta\delta_a\ \Delta\delta_r]'$ consists of control surfaces actuators and throttle inputs respectively as: elevator angle, throttle opening, aileron angle and rudder angle. $\boldsymbol{A}$ and $\boldsymbol{B}$ are state matrix and input matrix respectively. After decoupling the lateral and the longitudinal channel, we have

$$\begin{aligned}\boldsymbol{x}_{\text{lon}}(k+1)&=\boldsymbol{A}_{\text{lon}}\boldsymbol{x}_{\text{lon}}(k)+\boldsymbol{B}_{\text{lon}}\boldsymbol{u}_{\text{lon}}(k)\\ \boldsymbol{y}_{\text{lon}}(k)&=\boldsymbol{C}_{\text{lon}}\boldsymbol{x}_{\text{lon}}(k)\end{aligned}\tag{9}$$

$$\begin{aligned}\boldsymbol{x}_{\text{lat}}(k+1)&=\boldsymbol{A}_{\text{lat}}\boldsymbol{x}_{\text{lat}}(k)+\boldsymbol{B}_{\text{lat}}\boldsymbol{u}_{\text{lat}}(k)\\ \boldsymbol{y}_{\text{lat}}(k)&=\boldsymbol{C}_{\text{lat}}\boldsymbol{x}_{\text{lat}}(k)\end{aligned}\tag{10}$$

Here the longitudinal state variable is

$$\boldsymbol{x}_{\text{lon}}=[\ \Delta\upsilon\quad\Delta\alpha\quad\Delta q\quad\Delta\theta\quad\Delta H\ ]'$$

and the longitudinal control input is

$$\boldsymbol{u}_{\text{lon}}=[\ \Delta\delta_e\ \ \Delta\delta_T]'$$

whereas the lateral state variable is

$$\boldsymbol{x}_{\text{lat}}=[\ \Delta\beta\ \ \Delta p\ \ \Delta r\ \ \Delta\phi\ \ \Delta\psi\ \ Y\ ]$$

and the lateral control input is

$$\boldsymbol{u}_{\text{lat}}=[\ \Delta\delta_a\ \ \Delta\delta_r]'$$

where $\boldsymbol{A}_{\text{lon}}$, $\boldsymbol{B}_{\text{lon}}$, $\boldsymbol{A}_{\text{lat}}$, $\boldsymbol{B}_{\text{lat}}$ are the coefficient matrices.

3.2 Longitudinal control system

The longitudinal control system tracks the ideal glide slope altitude by adjusting the elevator angle and the throttle input. The preview information for longitudinal preview controller is the ideal glide slope height H_c relative to the flight deck. To convert the longitudinal channel into a form like $\boldsymbol{G}$, we have to augment the preview information $H_c(k)$ to the longitudinal channel given in Eq.(9) and Eq.(10). Define

$$\boldsymbol{e}(k)=H_c(k)-\boldsymbol{y}_{\text{lon}}(k)\tag{11}$$

$$\hat{\boldsymbol{x}}(k)=[\ \boldsymbol{x}_{\text{lon}}(k)\quad\boldsymbol{e}(k)\ ]'\tag{12}$$

We obtain the following system

$$\hat{\boldsymbol{x}}(k+1)=\hat{\boldsymbol{A}}\hat{\boldsymbol{x}}(k)+\hat{\boldsymbol{B}}_1H_c(k)+\hat{\boldsymbol{B}}_2\boldsymbol{u}(k)\tag{13}$$

$$\hat{\boldsymbol{z}}(k)=\hat{\boldsymbol{C}}_1\hat{\boldsymbol{x}}(k)+\hat{\boldsymbol{D}}_{11}H_c(k)+\hat{\boldsymbol{D}}_{12}\boldsymbol{u}(k)\tag{14}$$

$$\hat{\boldsymbol{y}}(k)=\hat{\boldsymbol{C}}_2\hat{\boldsymbol{x}}(k)+\hat{\boldsymbol{D}}_{21}H_c(k)\tag{15}$$

where

$$\hat{\boldsymbol{A}}=\begin{bmatrix}\boldsymbol{A}_{\text{lon}}&0\\-\boldsymbol{C}_{\text{lon}}&0\end{bmatrix},\quad\hat{\boldsymbol{B}}_1=\begin{bmatrix}0\\\boldsymbol{I}\end{bmatrix},\quad\hat{\boldsymbol{B}}_2=\begin{bmatrix}\boldsymbol{B}_{\text{lon}}\\0\end{bmatrix}$$

$$\hat{\boldsymbol{C}}_1=\begin{bmatrix}0&\boldsymbol{I}\\0&0\end{bmatrix},\quad\hat{\boldsymbol{D}}_{11}=\begin{bmatrix}0\\0\end{bmatrix},\quad\hat{\boldsymbol{D}}_{12}=\begin{bmatrix}0\\\boldsymbol{I}\end{bmatrix}$$

$$\hat{\boldsymbol{C}}_2=\begin{bmatrix}\boldsymbol{I}&0\\0&0\end{bmatrix},\quad\hat{\boldsymbol{D}}_{21}=\begin{bmatrix}0\\\boldsymbol{I}\end{bmatrix}$$

This is now a plant similar to general linearized discrete plant of the form $\boldsymbol{G}$. Similar to the process explained in Section 2.2, the delay line state can be augmented as $\chi_{\text{lon}}(k)=[\ \hat{\boldsymbol{x}}'(k)\ \boldsymbol{x}_d'(k)\ ]'$. Define

$$\overline{\boldsymbol{A}}_{\text{lon}}=\begin{bmatrix}\hat{\boldsymbol{A}}&\hat{\boldsymbol{B}}_1\boldsymbol{C}_p\\0&\boldsymbol{A}_p\end{bmatrix},\quad\overline{\boldsymbol{B}}_{\text{lon1}}=\begin{bmatrix}0\\\boldsymbol{B}_p\end{bmatrix},\quad\overline{\boldsymbol{B}}_{\text{lon2}}=\begin{bmatrix}\hat{\boldsymbol{B}}_2\\0\end{bmatrix}$$

$$\overline{\boldsymbol{C}}_{\text{lon1}}=\begin{bmatrix}\hat{\boldsymbol{C}}_1&\hat{\boldsymbol{D}}_{11}\boldsymbol{C}_p\end{bmatrix},\quad\overline{\boldsymbol{D}}_{\text{lon11}}=[0]$$

So, the full information version of longitudinal channel is given as

$$\boldsymbol{P}_{\text{lon}}=\begin{bmatrix}\overline{\boldsymbol{A}}_{\text{lon}} & \overline{\boldsymbol{B}}_{\text{lon1}} & \overline{\boldsymbol{B}}_{\text{lon2}}\\ \overline{\boldsymbol{C}}_{\text{lon1}} & \overline{\boldsymbol{D}}_{\text{lon11}} & \overline{\boldsymbol{D}}_{\text{lon12}}\\ \boldsymbol{I} & 0 & 0\\ 0 & \boldsymbol{I} & 0\end{bmatrix} \tag{16}$$

Assuming $\boldsymbol{P}_{\text{lon}}$ satisfies assumptions (1)—(3), the corresponding DARE similar to Eq.(5) can be solved to obtain H_∞ controller $\boldsymbol{K}_{\text{lon}}$ for a norm γ, as shown earlier. The closed loop transfer function (Fig.3) can be obtained by the linear fractional transformation $F_l(\boldsymbol{P}_{\text{lon}},\boldsymbol{K}_{\text{lon}})$.

$$\boldsymbol{z}=F_l(\boldsymbol{P}_{\text{lon}},\boldsymbol{K}_{\text{lon}})H_c \tag{17}$$

If we partition $\boldsymbol{P}_{\text{lon}}$ as

$$\boldsymbol{P}_{\text{lon}}=\begin{bmatrix}P_{11} & P_{12}\\ P_{21} & P_{22}\end{bmatrix} \tag{18}$$

then

$$F_l(\boldsymbol{P}_{\text{lon}},\boldsymbol{K}_{\text{lon}})=\boldsymbol{P}_{11}+\boldsymbol{P}_{12}(\boldsymbol{I}-\boldsymbol{K}_{\text{lon}}\boldsymbol{P}_{22})^{-1}\boldsymbol{K}_{\text{lon}}\boldsymbol{P}_{21} \tag{19}$$

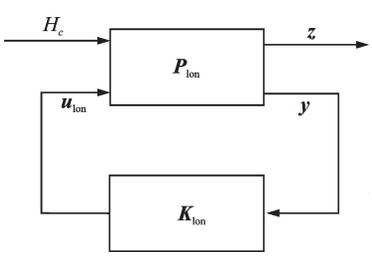

Fig.3 Longitudinal channel closed loop

The minimization of the following cost function

$$J_\infty(\boldsymbol{K}_{\text{lon}})=\|F_l(\boldsymbol{P}_{\text{lon}},\boldsymbol{K}_{\text{lon}})\|_\infty\leqslant\gamma \tag{20}$$

ensures the robustness properties of the H_∞ controller whereas the added preview improves the tracking and responsiveness of the resulting controller.

For the preview length to be N, the H_∞ preview controller has the form

$$\Delta\boldsymbol{u}_{\text{lon}}=K_x\boldsymbol{x}_{\text{lon}}(k)+K_e e_{\text{lon}}(k)+\sum_{i=1}^{N}K_H(i)H_c(k+i)$$

3.3 Lateral control system

For a successful landing, the aircraft has to follow a reference glide trajectory. Lateral control system ensures the aircrafts stay on the center line leading to the touchdown point and correct any errors in the azimuthal angle. This is achieved by controlling the roll angle using the aileron and rudder to stay on the trajectory. Reference signal available for preview is the lateral bias Y_c. Similar to the longitudinal control system design, we have to augment the preview information $Y_c(k)$ to the lateral channel and convert the resulting system to standard H_∞ framework by further augmenting the delay line as. The H_∞ lateral preview control input has the following form

$$\Delta\boldsymbol{u}_{\text{lat}}=K_x\boldsymbol{x}_{\text{lat}}(k)+K_e e_{\text{lat}}(k)+\sum_{i=1}^{N}K_Y(i)Y_c(k+i)$$

4 Simulation Results

For simulation and verification purposes, a linearized model of F/A-18 trimmed at carrier landing phase was used. Trim state values are shown in Table 1.

Table 1 Trim state values

Parameter	Value
V/(m·s^{-1})	69.3
α/(°)	8.5
q/((°)·s^{-1})	0
θ/(°)	5
β/(°)	0
p/((°)·s^{-1})	0
r/(°)	0
φ/(°)	0
ψ/(°)	0
δ_e/(°)	−3.17
δ_T/%	0.43
δ_a/(°)	0
δ_r/(°)	0
H/m	240.7

The linearized equilibrium state model of the final-approach dynamics has the following form

$$\boldsymbol{x}(k+1)=\boldsymbol{A}\boldsymbol{x}(k)+\boldsymbol{B}\boldsymbol{u}(k) \tag{21}$$

where state

$$\boldsymbol{x}=[\Delta V\ \Delta\alpha\ \Delta q\ \Delta\theta\ \Delta\beta\ \Delta p\ \Delta r\ \Delta\phi\ \Delta\psi\ \Delta H\ \Delta Y]'$$

and input

$$\boldsymbol{u}=[\Delta\delta_e\ \Delta\delta_T\ \Delta\delta_a\ \Delta\delta_r]'$$

This state space model can be decoupled into lateral and longitudinal models.

4.1 F/A-18 longitudinal model

After discretization with a sampling time of 0.01 s, the state matrices of longitudinal approach

dynamics are given as follows

$$\boldsymbol{A}_{\text{lon}}=\begin{bmatrix} 0.089\,5 & 3.370\,3 & -0.025\,4 & -32.111\,2 & 0 \\ -0.001\,2 & -0.587\,1 & 0.990\,8 & 0.008\,5 & 0 \\ 0 & -0.300\,1 & -0.184\,5 & 0 & 0 \\ 0 & 0 & 1 & 0 & 0 \\ 0 & \dfrac{-70}{0.304\,8} & 0 & \dfrac{70}{0.304\,8} & 0 \end{bmatrix},\quad \boldsymbol{B}_{\text{lon}}=\begin{bmatrix} -0.004\,5 & 18.803\,7 \\ -0.001\,4 & -0.012\,3 \\ -0.026\,0 & 0 \\ 0 & 0 \\ 0 & 0 \end{bmatrix}$$

4.2 F/A-18 lateral model

Similarly, after discretization with a sampling time of 0.01 s, the state matrices of lateral approach dynamics are given as follows

$$\boldsymbol{A}_{\text{lat}}=\begin{bmatrix} -0.103\,5 & 0.147\,4 & -0.987\,2 & 0.141 & 0 & 0 \\ -4.068\,4 & -1.251\,4 & 0.584\,6 & 0 & 0 & 0 \\ 0.558\,3 & -0.009 & -0.079\,1 & 0 & 0 & 0 \\ 0 & 0 & 1 & 0 & 0 & 0 \\ 0 & 0 & 0 & 0 & \dfrac{70}{0.304\,8} & 0 \end{bmatrix},\quad \boldsymbol{B}_{\text{lat}}=\begin{bmatrix} 0 & 0.000\,4 \\ 0.047 & 0.007\,4 \\ -0.000\,7 & 0.005\,8 \\ 0 & 0 \\ 0 & 0 \\ 0 & 0 \end{bmatrix}$$

4.3 Controller response

For simulating automatic carrier landing conditions, Fig.4 and Fig.5 show the height response and the velocity response with a longitudinal controller, and Fig.6 shows the deviation response with a lateral controller, both of them are based on H_∞ preview control which has a preview length of 15. It can be clearly seen that the controller reacts to the future change in input for a better tracking performance. The height response greatly tracks a glide slope as a ramp signal, and the lateral deviation immediately converges to zero in 10 s. All of them clearly depict that the system is acting in advance to be ready for the incoming reference signal.

For comparison, Figs. 7—9 show the corresponding responses with controllers based on PID control. It exhibits that the superior control performance of preview control is evident. Owing to the anticipative control effort, preview controller provides a better transient response and quicker tracking with lower tracking error over the transient stage. The maximum tracking error for longitudinal channel with preview is less than that of PID control.

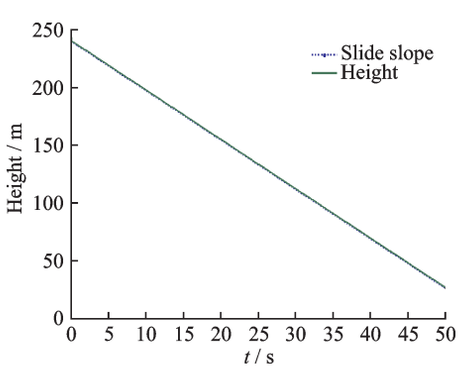

Fig.4 Height response, H_∞ preview control

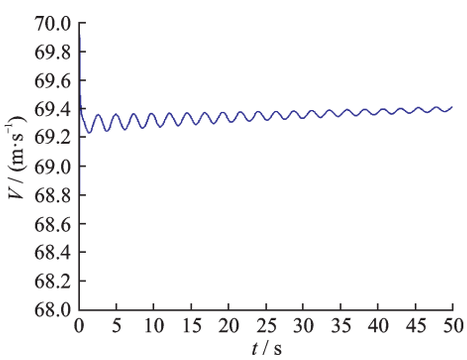

Fig.5 Velocity response, H_∞ preview control

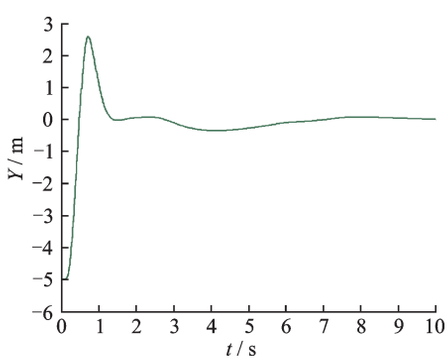

Fig.6 Lateral deviation response, H_∞ preview control

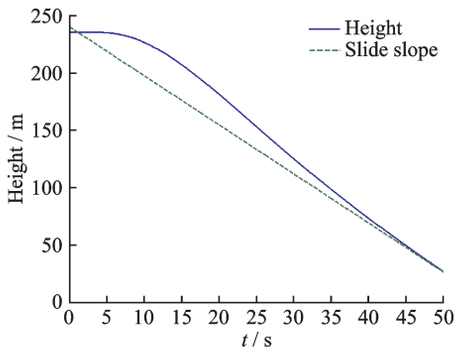

Fig.7 Height response, PID control

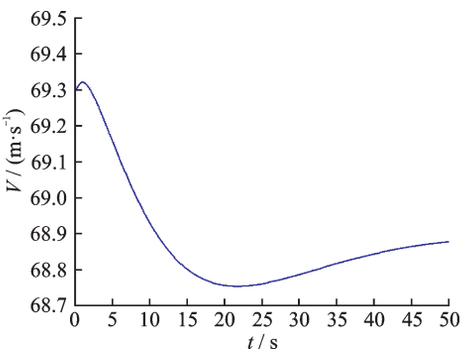

Fig.8 Velocity response, PID control

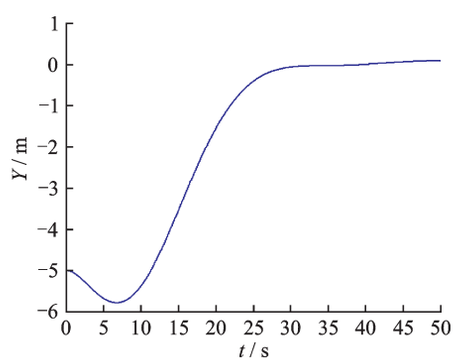

Fig.9 Lateral deviation response, PID control

5 Conclusions

Conventional control methods are causal and cannot make use of future information. Preview control provides us a methodology to develop controllers that can utilize future information of references and disturbances to further improve the controller performance and react a priori. H_∞ preview control combines the robustness and disturbance rejection properties of H_∞ feedback control and look ahead properties of feedforward preview control. Most of the work in H_∞ preview control was scattered over various theoretical results, hence, the practicality from the engineering perspective was low until recently[23]. This paper combined the results in order to provide a generic framework and flow for synthesizing preview controllers for ACLS control problem. The process of adding preview to a traditional ACLS plant model and solving the resulting preview control problem using H_∞ control theory was laid out. Moreover, the procedure was verified using the example of F/A-18 carrier landing problem. Results showed that H_∞ preview control can provide superior tracking performance compared to conventional PID control.

References

[1] ZHEN Z Y, ZHANG Z B, ZHANG J H. Guidance and control techniques of carrier-based aircraft for automatic carrier landing[J]. Transactions of Nanjing University of Aeronautics and Astronautics, 2017, 34(6): 600-608.

[2] BOSKOVIC J, REDDING J. An autonomous carrier landing system for unmannned aerial vehicles [C]// AIAA Guidance, Navigation, and Control Conference. Chicago: AIAA, 2009: 62-64.

[3] STORVIK M. Guidance system for automatic approach to a ship[D]. Norway: Norwegian University of Science and Technology, 2003.

[4] DURAND T S, WASICKO R J. Factors influencing glide path control in carrier landing[J]. Journal of Aircraft, 1967, 4(2): 146-158.

[5] XIA G, DONG R, XU J, et al. Linearized model of carrier-based aircraft dynamics in final-approach air condition[J]. Journal of Aircraft, 2015, 53(1):33-47.

[6] STEINBERG M. Development and simulation of an F/A-18 fuzzy logic automatic carrier landing system [C]//Second IEEE International Conference on Fuzzy Systems. [S.l.]: IEEE, 1993: 797-802.

[7] SKULSTAD R, SYVERSEN CL, MERZ M, et al. Net recovery of UAV with single-frequency RTK GPS[C]//IEEE Aerospace Conference.[S.l.]:IEEE, 2015: 1-10.

[8] ZHEN Z Y, MA K, BHATIA AK . Automatic carrier landing control for unmanned aerial vehicles based on preview control[J]. Transactions of Nanjing University of Aeronautics and Astronautics, 2017, 34(4): 413-419.

[9] TOMIZUKA M. Optimal continuous finite preview problem[J]. IEEE Transactions on Automatic Control, 1975, 20(3): 362-365.

[10] BIRLA N, SWARUP A. Optimal preview control: A review[J]. Optimal Control Applications and Methods, 2015, 36(2): 241-268.

[11] YU X, LIAO F C, SHI M K. Preview control with imaginary input[J]. China Journal of Basic Science and Engineering, 1998, 6(3): 319-326.

[12] LIAO Fucheng, TSUCHIYA T, TADASHI E, et al. Unified handling of optimal preview servo systems and optimal preview FF compensating systems[J]. Acta Automatica Sinica, 1998, 24(5): 640-646.

[13] KRISTALNY M, MIRKIN L. On the H_2 two-sided model matching problem with preview[J]. IEEE Transactions on Automatic Control, 2012, 57(1): 204-209.

[14] TAN Y, FENG L. Digital optimal preview control of trajectory tracking based on trajectory error area[J]. Chinese Journal of Scientific Instrument, 2004, 25(1): 86-89. (in Chinese)

[15] SHI Q S, LIAO F C. Design of an optimal preview controller for linear discrete-time multirate systems with state-delay[J]. Journal of University of Science and Technology Beijing, 2011, 33(3): 363-375.

[16] ZOU Q, DEVASIA S. Precision preview-based stable-inversion for nonlinear nonminimum-phase systems: The VTOL example[J]. Automatica, 2007, 43(1): 117-127.

[17] LIAO F, TAKABA K, KATAYAMA T, et al. Design of an optimal preview servomechanism for discrete-time systems in a multirate setting[J]. Dynamics of Continuous Discrete and Impulsive Systems Series B, 2003, 10: 727-744.

[18] LIAO Fucheng, LIU Heping. Design of an optimal preview controller for a kind of discrete-time system with time-delay[J]. Journal of University of Science and Technology Beijing, 2008, 30(4): 452-460.

[19] XU Y, LIAO F. Design of the optimum preview controller for a class of state-delay systems[J]. Journal of University of Science and Technology Beijing, 2006, 28(4): 403-408.

[20] TAKABA K. A tutorial on preview control systems [C]// SICE 2003 Annual Conference.[S.l.]: IEEE, 2003: 1388-1393.

[21] TOMIZUKA M. The optimal finite preview problem and its application to man-machine systems[D]. Boston, USA: Massachusetts Institute of Technology, 1973.

[22] HAZELL A, LIMEBEER D J N. An efficient algorithm for discrete-time H_∞ preview control[J]. Automatica, 2008, 44(9): 2441-2448.

[23] HAZELL A. Discrete-time optimal preview control [D]. London, UK: Imperial College London, 2008.

[24] GREEN M, LIMEBEER D J N. Linear robust control[M].New Jersey, USA: Prentice Hall, 2012.

[25] URNES J M, MOOMAW R F, HUFF R W. H-dot automatic carrier landing system for approach control in turbulence[J]. Journal of Guidance, Control, and Dynamics, 1981, 4(2): 177-183.

Acknowledgements This work was supported by the National Natural Science Foundation of China (Nos. 61973158, 61304223, 61673209), the Aeronautical Science Foundation (NO. 2016ZA52009), the Fundamental Research Funds for the Central Universities (Nos. NS2017015, NJ20170005).

Authors Mr. **FARHAN Masood** is a graduate student at College of Automation Engineering, Nanjing University of Aeronautics and Astronautics. His research interests include preview control, robust control and advanced flight control systems.

Ms. **XUE Yixuan** is studying in College of Automation Engineering, Nanjing University of Aeronautics and Astronautics for doctor's degree. Her research interests include fault tolerant control and preview control.

Prof. **ZHEN Ziyang** received his Ph.D. degree from College of Automation Engineering, Nanjing University of Aeronautics and Astronautics in 2010. He had been working at the University of Virginia, U.S.A. as a visiting scholar from February 2015 to February 2016. Currently, he is working at Nanjing University of Aeronautics and Astronautics as a professor. His research interests include advanced flight control, information fusion control and preview control.

Ms. **YANG Liuqing** is a graduate student at College of Automation Engineering, Nanjing University of Aeronautics and Astronautics. Her research interests include advanced flight control and adaptive control.

Author contributions Mr. **FARHAN Masood** contributed to the discussion and background of the study, designed the study proposal and wrote the manuscript. Ms. **XUE Yixuan** provided the simulation experiments and revised paper. Prof. **ZHEN Ziyang** provided technical and financial support for this research. Ms. **YANG Liuqing** supplied the establishment of aircraft model and landing model.

Competing interests The authors declare no competing interests.

(Production Editor: Sun Jing)